308

Investigating the Mechanisms of HIV-1 Latency by High Resolution Microscopy

Luca Sardo[1], Angel Lin[1], Svetlana Khakhina[1], Lucas Beckman[1], Luis Ricon[1], Weam Elbezanti[1], Tara Jaison[1], Harshad D. Vishwasrao[2], Hari Shroff[3], Christopher J. Janetopoulos[1] and Zachary A. Klase[1]

1 Department of Biological Sciences, McNeil Science and Technology Center, University of the Sciences, Philadelphia, PA
2 Advanced Imaging and Microscopy Resource, NIH, Bethesda, MD
3 Section on High Resolution Optical Imaging, National Institute of Biomedical Imaging and Bioengineering, NIH, Bethesda, MD

Background. Biochemical evidence demonstrated that the state of chromatin condensation and the recruitment of regulators of transcription on the HIV-1 LTR can control virus latency during antiretroviral therapy. However, our understanding of these mechanisms in a living cell are limited. Optical microscopy can visualize events in real-time at a single cell level, but the cell body and organelles can hamper the staining and visualization of the nucleus. In fact, high resolution microscopy techniques require fixation of the sample or expression of exogenous fluorescently tagged proteins, which are respectively limited by loss of time resolution and potential artifacts associated with over-expression. Therefore, high resolution microscopy tools to study endogenous nuclear events in real-time are in need.

Methods. Transcriptionally competent nuclei were isolated from cell line models of HIV-1 latency and immunostained without fixation for endogenous chromatin markers and chromatin modifying enzymes. Latency reversing agents (LRAs) were supplemented to isolated nuclei to induce chromatin remodeling. State of the art confocal and structural illumination multicolor live microscopy coupled with computational image analysis were used to visualize and quantify chromatin changes in real-time.

Results. The spatial organization and accumulation of novel HIV-1 LTR transcription regulators RUNX1 and STAT5 proteins was observed in response to LRAs treatment at unprecedented resolution in unfixed specimens. Microscopy observations were validated by flow cytometry and biochemical assays. In similar experiments we employed CRISPR/dCas9-SunTag to visualize the HIV-1 LTR and to study its association with chromatin markers in response to virus reactivation.

Conclusions. We have developed a high resolution, live imaging approach to investigate the in-vivo molecular mechanisms involved in HIV-1 transcriptional latency.

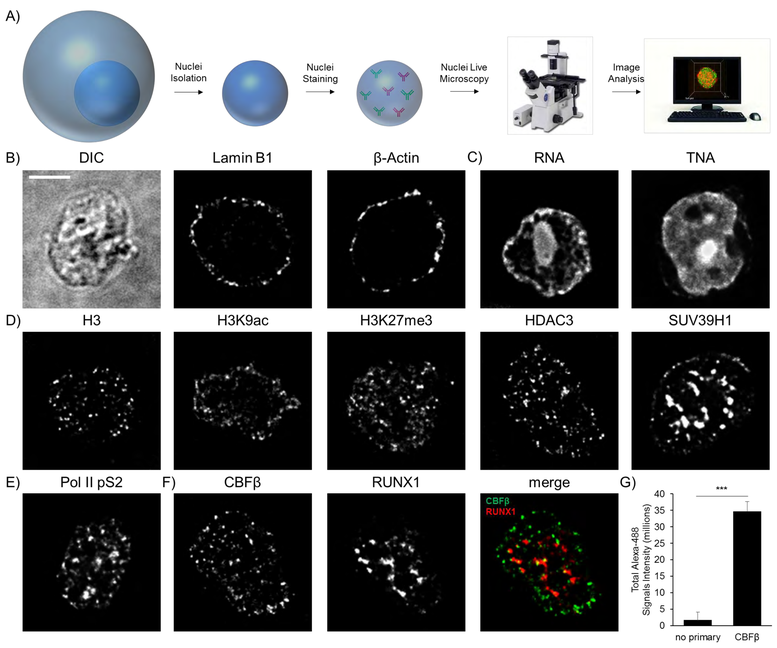


Figure 1. Visualization of endogenous nuclear targets in isolated nuclei. Nuclei isolated from TZM-bl cells were stained without fixation and imaged by confocal microscopiny. A) Experimental workflow. B) Differential interference contrast image of a representative nucleus (DIC) and immunostaining of structural proteins, lamin B1 and β-actin. C) RNA and total nucleic acids (TNA) stains. D) Immunostaining of the histone code: unmodified histone 3 (H3), acetylated and methylated histone H3 (H3K9ac and H3K27me3), histone deacetylase 3 (HDAC3), histone-lysine N-methyltransferase SUV39H1. E) Immunostaining of the phosphorylated RNA polymerase II (Pol II pS2) and F) proteins of the core binding factor, CBFβ (green) and RUNX1 (red). G) Total signal intensity averaged from nuclei stained for CBFβ and from control nuclei stained with secondary antibody only (no-primary, n=3 per condition). Asterisks indicate differences statistically significant between conditions shown as *** ($P \leq 0.001$). Deconvolved confocal equatorial z-series of representative nuclei are shown. Scale bar, 5 µm.

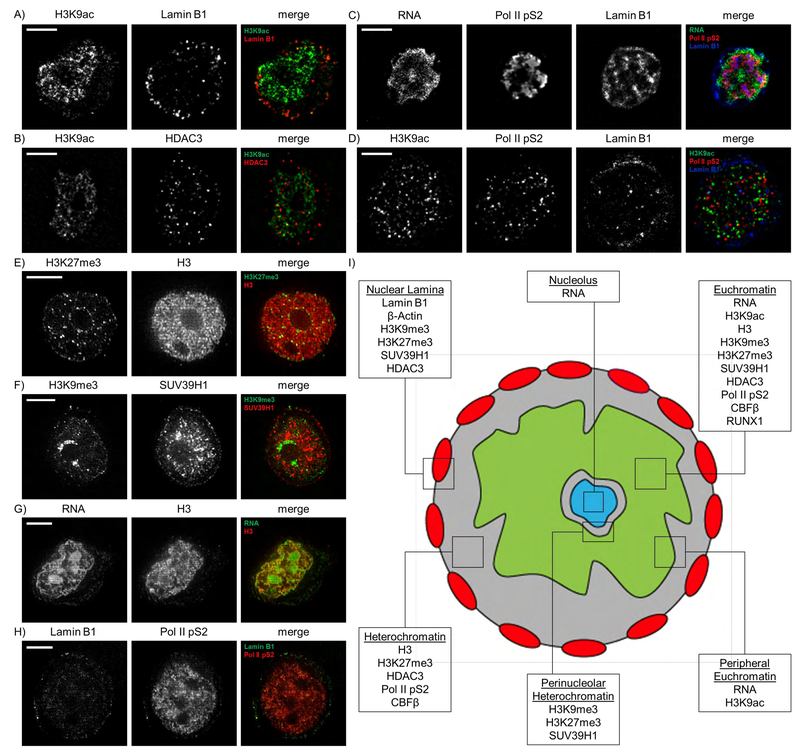


Figure 2. Mapping the location of endogenous nuclear proteins and nucleic acids by confocal and super resolution microscopy. Nuclei isolated from TZM-bl cells were co-stained for the given nuclear targets and imaged by confocal microscopy (A-D) and iSIM (E-H). I) Representative map of nuclear proteins and nucleic acids location in the nucleus as determined by these studies. Deconvolved confocal equatorial z-series of representative nuclei are shown. Scale bars, 5 µm.

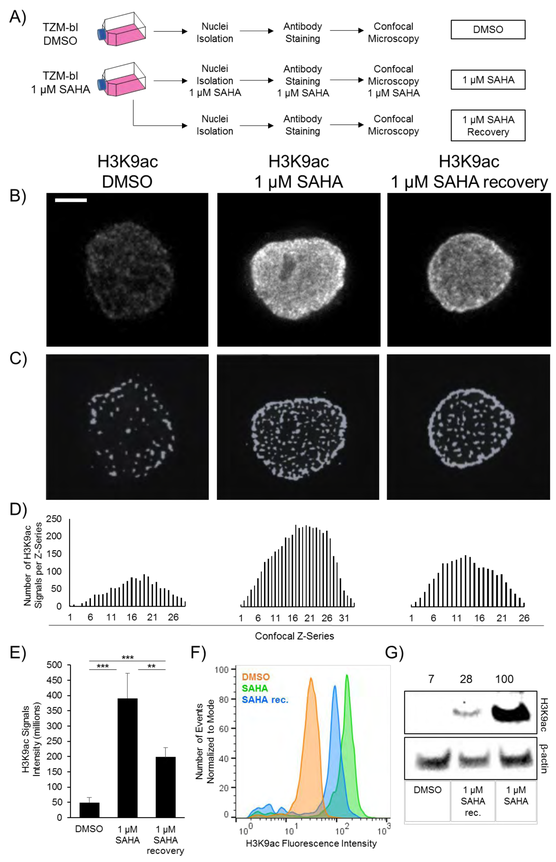


Figure 3. Examination of histone deacetylase inhibition in isolated nuclei. A) Experimental workflow. TZM-bl cells were cultured for 48 hours in media containing 1 µM SAHA and processed for nuclei isolation, staining and microscopy (DMSO, untreated control). B) Representative confocal equatorial z-series of nuclei stained for acetylated H3 (H3K9ac) and C) software assisted identification of H3K9ac fluorescent signals detected in images shown in panel B. D) Levels of H3K9ac signals in confocal z-series. E) Quantification of the total H3K9ac nuclear signals fluorescence (n=3 per condition). F) Quantification of H3K9ac fluorescence in isolated nuclei by flow cytometry. G) Quantification of H3K9ac protein amount by Western blot. Scale bar, 5 µm. Statistically significant differences between conditions are shown as ** ($P \leq 0.01$) and *** ($P \leq 0.001$).

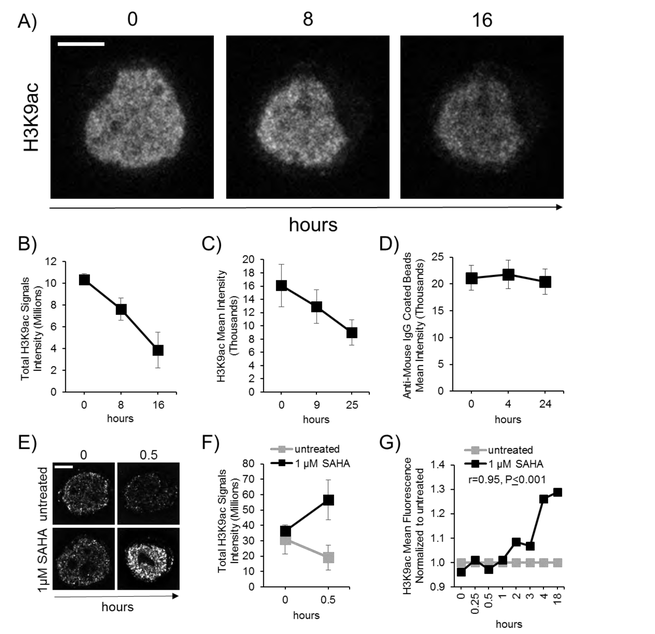


Figure 4. Visualization of histone acetylation in real-time. A) Acetylated H3 visualized at single nucleus level during a time-lapse experiment in the absence of SAHA and B) quantification of the average total H3K9ac signals fluorescence (n=3 per time point). C) H3K9ac average fluorescence emitted from isolated nuclei and measured by flow cytometry over time (500 nuclei per time point). D) Fluorescence from H3K9ac stained IgG coated beads measured by flow cytometry over time (2000 beads per time point). E) Time-lapse visualization of H3K9ac in representative nuclei treated ex-vivo with 1 µM SAHA and F) relative fluorescence quantification (n=3 per time point and per condition). G) H3K9ac fluorescence after 1 µM SAHA treatment measured by isolated nuclei flow cytometry (3000 nuclei per time point and per condition). Confocal equatorial z-series of representative TZM-bl nuclei are shown (panel E: images deconvolved). Scale bar, 5 µm.

Contact Information

Correspondence:
l.sardo@usciences.edu
z.klase@usciences.edu

Twitter:
@drlucasardo
@ProfKlase

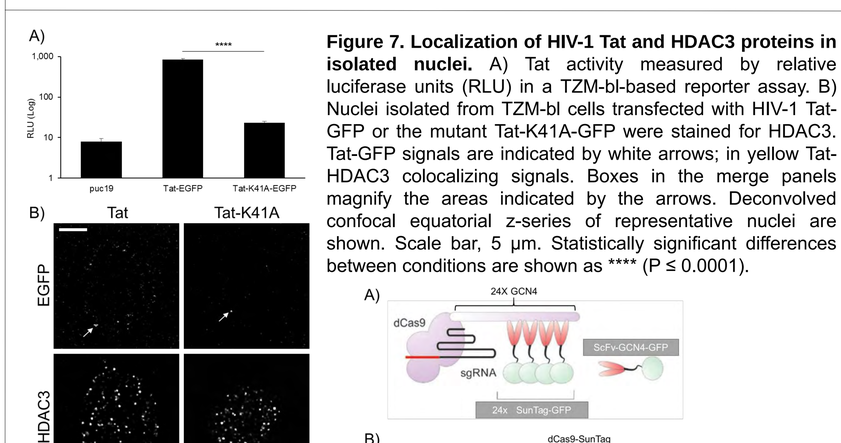


Figure 5. Visualization of chromatin reorganization in isolated nuclei. A) Nuclei isolated from TZM-bl cells treated with 1 µM SAHA were stained for acetylated H3 (H3K9ac, green), phosphorylated RNA polymerase II (Pol II pS2, red) and lamin B1 (blue). DMSO, untreated control. Scale bar, 5 µm. B) Localization maps of images in panel A showing the position of H3K9ac (green dots), Pol II pS2 (red dots) and H3K9ac/Pol II pS2 colocalizing signals (yellow dots). C) Quantification of H3K9ac and Pol II pS2 colocalization percentage relative to the nuclei shown in panel A. D) Total number of H3K9ac and E) Pol II pS2 and F) H3K9ac/Pol II pS2 colocalizing signals detected in equatorial z-series (DMSO, n=4; SAHA, n=3). Statistically significant differences between conditions are shown as * ($P \leq 0.05$) and ** ($P \leq 0.01$).

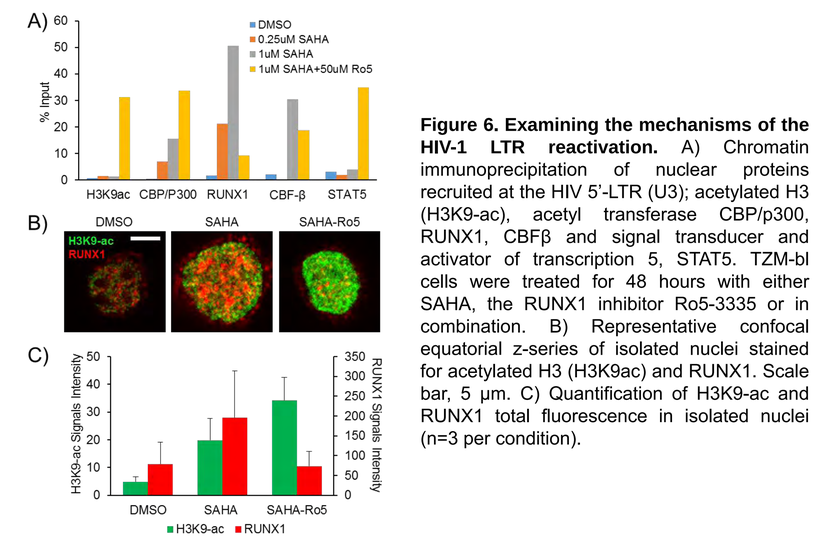


Figure 6. Examining the mechanisms of the HIV-1 LTR reactivation. A) Chromatin immunoprecipitation of nuclear proteins recruited at the HIV 5'-LTR (U3); acetylated H3 (H3K9-ac), acetyl transferase CBP/p300, RUNX1, CBFβ and signal transducer and activator of transcription 5, STAT5. TZM-bl cells were treated for 48 hours with either SAHA, the RUNX1 inhibitor Ro5-3335 or in combination. B) Representative confocal equatorial z-series of isolated nuclei stained for acetylated H3 (H3K9-ac) and RUNX1. Scale bar, 5 µm. C) Quantification of H3K9-ac and RUNX1 total fluorescence in isolated nuclei (n=3 per condition).

Figure 7. Localization of HIV-1 Tat and HDAC3 proteins in isolated nuclei. A) Tat activity measured by relative luciferase units (RLU) in a TZM-bl-based reporter assay. B) Nuclei isolated from TZM-bl cells transfected with HIV-1 Tat-GFP or the mutant Tat-K41A-GFP were stained for HDAC3. Tat-GFP signals are indicated by white arrows; in yellow Tat-HDAC3 colocalizing signals. Boxes in the merge panels magnify the areas indicated by the arrows. Deconvolved confocal equatorial z-series of representative nuclei are shown. Scale bar, 5 µm. Statistically significant differences between conditions are shown as **** ($P \leq 0.0001$).

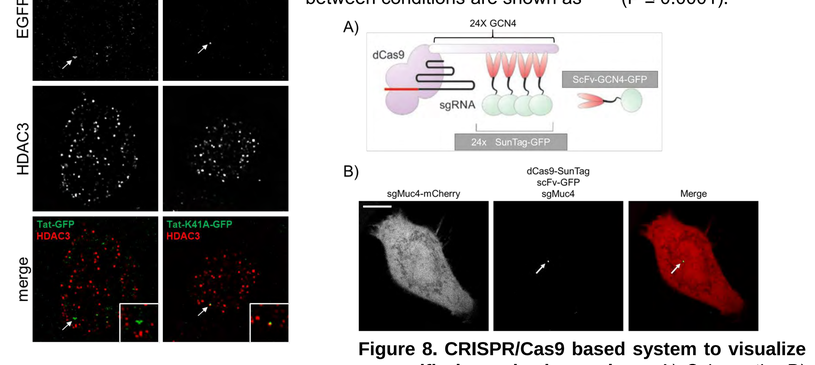


Figure 8. CRISPR/Cas9 based system to visualize a specific locus in the nucleus. A) Schematic. B) Representative transfected TZM-bl cell. Arrow indicates SunTag-GFP signals. Scale bar, 10 µm.

Conclusions

- To our knowledge, ours is the first report that provides high resolution visualization of endogenous nuclear proteins and nucleic acids in an unfixed sample.
- We generated an extensive localization map of structural proteins, proteins of the histone code and transcription factors in isolated nuclei.
- We investigated the dynamics of chromatin remodeling, RNA transcription, viral proteins function and nuclear architecture in real-time.
- We are developing a CRISPR/Cas9 system to localize the HIV-1 LTR in nuclei.

Financial Support

This work was supported by University of the Sciences internal funds and a grant from the WW Smith Charitable trust to Z.K. and C.J. The authors declare no conflict of interest.